MATHEMATICS DEPARTMENT

On Spurious Asymptotic Numerical Solutions of 2×2 Systems of ODEs[1]

P.K. Sweby
&
H.C. Yee[2]

Numerical Analysis Report 7/91

October 1991

UNIVERSITY OF READING

[1]The majority of this work was performed whilst the first author was a visiting scientist at the NASA Ames Research Center.

[2]Staff Scientist, Fluid Dynamics Division, NASA Ames Research Center, Moffett Field, CA 9 035,USA

The phenomenon that the asymptotic behaviour of a nonlinear differential equation and its discretized counterpart can have different dynamical behavior was not uncovered fully until recently. In our earlier work we discussed some of the differences between the dynamics of scalar first-order autonomous nonlinear OD s and commonly used OD solvers. In this report

1 Introduction

Until recently it was not fully appreciated that the dynamical behaviour of a numerical discretisation of a non-linear differential equation is not necessarily the same as the dynamics of the original equation itself. Iserles [11] showed that whilst linear multistep methods for solving OD s possess only the fixed points of the original differential equations, popular Runge-Kutta methods may exhibit additional, spurious, fixed points. It has been demonstrated (see for example [17, 7, 19] for the scalar case, and [12, 13] for nonlinear reaction-convection model equations) that such spurious fixed points may be stable below the linearised stability limit of the scheme and, although Humphries [10] has recently shown that if such stable spurious fixed points exist as the time-step approaches zero they must either approach a true fixed point or become unbounded, these spurious features may greatly affect the dynamical behaviour of the numerical solution in practice due to the use of a finite timestep. Indeed this will be the case not only for stable spurious fixed points but also for unstable spurious fixed points and spurious higher order features such as period 2 solutions or even chaos which can be admitted by even the Linear Multistep methods, including the simple uler scheme. (Hairer *et al* [9] have studied classes of "regular" methods which do not exhibit spurious period one or period two fixed points.)

In [17, 7, 19] we demonstrated the occurrence of spurious fixed points for scalar OD s when discretised by various numerical schemes. In this report and [18] we investigate, largely numerically, the dynamics of numerical discretisations of 2×2 systems of first-order autonomous nonlinear OD s, illustrating how wrong, non-convergent or no solutions may be obtained for the discretised equation due to spurious fixed points, limit cycles and numerical basins of attraction respectively. As in the scalar case these phenomena may occur below or very closed to the linearised stability limits of the schemes (itself not always easily calculated). Our ultimate goal is to study and fully appreciate the dynamics of discretisations of PD s and how it relates to the dynamics of the PD s themselves, in particular where time-stepping techniques are used to reach a steady-state; preliminary work on this has already commenced ([6, 12, 13]). It is important to remember that not only the discretisations but also preconditioners and relaxation techniques may also modify the dynamics of the original PD .

In Section 2 we briefly review some basic bifurcation theory before introducing our test cases in Section 3. In Section 4 we proceed to investigate the dynamics of various Runge-Kutta methods applied to our model equations, summarizing our findings in Section 5. Finally, in the Appendix, we describe the techniques used to obtain our detailed pictures of solution orbits and basins of attraction on a Connection Machine CM2.

Before embarking on a description of the systems which we will use as illustrations and the numerical methods which we shall apply to them we review some of the basic theory of fixed points and their bifurcations (see for example [8, 4] for a detailed account).

E

E

E ^{2}

E

$J(\mathbf{u}_E)t$ $_0$

λt

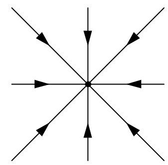

such a scheme in the form

$$\mathbf{u}^{n+1} = \mathbf{u}^n + r\mathbf{G}(\mathbf{u}^n) \tag{6}$$

where superscripts denote the time level (e.g. $n\Delta t$) and we use r to represent the time-step Δt but allowing it to include any constant scaling factors present in $\mathbf{F}$. The vector function $\mathbf{G}$ is assumed consistent with the OD in the sense that $\mathbf{F}(\mathbf{u}_E) = 0 \Rightarrow \mathbf{G}(\mathbf{u}_E) = 0$, i.e. that fixed points of the OD are fixed points of the scheme. Note that in general the converse does not hold, the scheme possessing fixed points which are not fixed points of the OD (see e.g. [11, 19, 17, 7]). It is this feature which forms the core of our work.

The scheme (6) has fixed points $\mathbf{G}(\mathbf{u}_N) = 0$ which may be true fixed points of (1) $\mathbf{u}_E$ or spurious fixed points $\mathbf{u}_S$. If we perform a perturbation analysis on (6) about $\mathbf{u}_N$ then we obtain

$$\boldsymbol{\epsilon}^{n+1} = \boldsymbol{\epsilon}^n + r\frac{\partial \mathbf{G}(\mathbf{u}_N)}{\partial \mathbf{u}}\boldsymbol{\epsilon}^n + O(\epsilon^2) \tag{7}$$

which, ignoring higher order terms, has solution

$$\boldsymbol{\epsilon}^{n+1} = (I + r\frac{\partial \mathbf{G}(\mathbf{u}_N)}{\partial \mathbf{u}})^{n+1}\boldsymbol{\epsilon}^0. \tag{8}$$

Therefore, for the numerical fixed point $\mathbf{u}_N$ to be stable the eigenvalues of the matrix (assuming $\partial\mathbf{G}(\mathbf{u}_N)/\partial\mathbf{u} \neq 0$)

$$(I + r\frac{\partial \mathbf{G}(\mathbf{u}_N)}{\partial \mathbf{u}}) \tag{9}$$

must lie inside the unit circle. As for the OD , the relative positioning of the eigenvalues (considering a 2×2 system) determines the type of fixed point. If both eigenvalues are real and both lie inside/outside the unit circle then the fixed point is a stable/unstable node. If one is inside the unit circle, the other outside, then the fixed point is a saddle and if they are complex then the fixed point is a spiral. The situation of eigenvalues on the unit circle (not varying with parameters of the system) is in general indeterminent.

When a fixed point of the discrete map becomes unstable, usually through variation of r, then one of three situations can occur. If the eigenvalue passing outside the unit circle is -1 then a “flip” or “period doubling” bifurcation occurs, however if the eigenvalue is $+1$ then the bifurcation is to another steady state. This bifurcation can either be transcritical (the branches extending both above and below the bifurcation in parameter space) or pitchfork (either subcritical or supercritical), the exact nature depending on higher order terms, see e.g. [7] or [17] for a scalar exposition. If the eigenvalues are complex then (with a few exceptions - see [8]) a Hopf bifurcation occurs. Again the reader is encouraged to refer to [8] and [4] for full details. The stability of bifurcation branches is established in a similar fashion as above, with usually only portions of the branches being stable.

Finally another feature which can arise (for both a system of OD s and their discretisation), usually as the result of a Hopf bifurcation, is a limit cycle where the map traverses a closed curve in phase space. In all but a few simple cases such limit cycles are beyond analysis.

In this present work we restrict ourselves to four non-linear systems of OD s to illustrate the modified dynamics of our OD solvers over the dynamics of the original differential equations. Two of these systems arise from the mathematical modelling of physical and biological processes, namely a damped pendulum and a simple model of predator-prey interaction in pop-

$2 \quad \frac{1}{2} \quad 3$

2

$\frac{3}{4} \quad 2$

$\frac{3}{4} \quad 2$

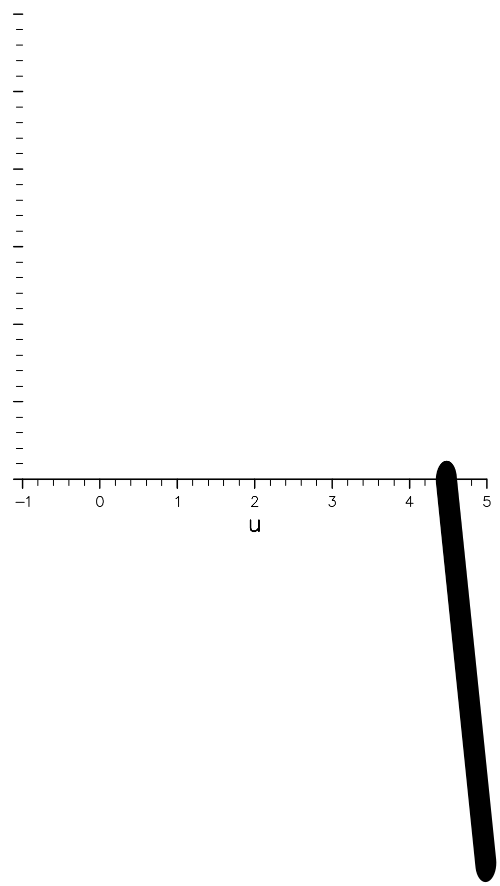
–1
0
1
2
3
4
5
u

fixed point	eigenvalues	type	eigenvectors
$((2 \quad +1) \quad 0)$	$\frac{-\beta\pm \quad \sqrt{\beta^2+4}}{2}$	Saddles	$(1 \quad {}_1)^T, \ (1 \quad {}_2)^T$
$(2 \quad \quad 0)$	$\frac{-\beta\pm \quad \sqrt{\beta^2-4}}{2}$	Stable Spirals $\quad 2$ Stable Nodes $\quad 2$	

Table 2: The fixed points of the Damped Pendulum equation.

Jacobian of this system is

$$= \begin{matrix} 0 & 1 \\ \cos(\quad) & \end{matrix} \tag{15}$$

which, at the fixed points, has eigenvalues

$$= \frac{\sqrt{\quad {}^2 \quad 4(\quad 1)^k}}{2} \tag{16}$$

If is odd then it is easily seen that the eigenvalues are of opposite sign and

$$^2 \qquad ^2$$

$$^2 \qquad ^2$$

$$\frac{\quad ^2}{\quad} \qquad ^2 \qquad ^2$$

^{2}

$$-$$

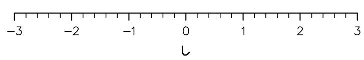

−3 −2 −1 0 1 2 3
ι

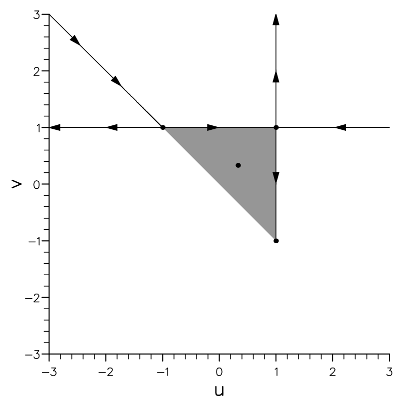

v
u
3
2
1
0
−1
−2
−3
−3
−2
−1
0
1
2
3

$\frac{1}{2}$

$-$

$-$

$-$

$-$

$-$

$-$

$-$

$-$

$-$

order schemes applied to some of our examples. Where rigorous analysis is impractical we have still been able to investigate the dynamics using numerical experiments. For this the NASA Ames Connection Machine CM2 was used which enabled vast numbers (typically 512^2) calculations to be performed in parallel, each calculation identical apart from either initial data or time-step parameter. It was therefore possible to obtain both full bifurcation diagrams in a ( ) plane and orbits with their basins of attraction in the been very selective in the results presented here, but even so the prescence and nature of spurious dynamical behaviour is evident.

4.1 The Predator Prey equations

Due to consistency, the fixed points of the OD s will also be fixed points of the Runge-Kutta schemes which we are considering. However, the stability (and type) of these essential fixed points of the schemes will depend on the parameter r, the stability condition for a k-th order Runge-Kutta method being ([14]) $|\mu| < 1$ where

$$\mu = 1 + r\lambda + \cdots + \frac{r^k \lambda^k}{k!} \tag{29}$$

and λ ranges over the eigenvalues of the Jacobian J of the system of OD s. (This expression arises from the fact that the scheme is a k-th order approximation to the OD s.) It is easily verified that if $\Re e(\lambda) > 0$ then $|\mu| > 1$ and so unstable fixed points of the OD s will not be stable fixed points of the scheme, although as we shall see their type may change.

For the uler scheme (23) the stability polynomial (29) is just $\mu = 1 + r\lambda$ and so we can use the eigenvalues from Table 1 to obtain the stability and type of each of the fixed points. For illustrative purposes we shall give the details for this simple case, however in general we shall just state the results, the analysis being straight forward (if tedious). We have therefore, for the fixed points of the uler scheme applied to the Predator Prey equations

$(0,0)$: $\mu_1 = 1 - 3r$, $\mu_2 = 1 - 2.1r$
Stable node $r \in (0, \frac{2}{3})$,
Saddle $r \in (\frac{2}{3}, \frac{2}{2.1} = 0.\dot{9}5238\dot{0})$
Unstable node $r > 0.\dot{9}5238\dot{0}$

$(1,0)$: $\mu_1 = 1 - 1.1r$, $\mu_2 = 1 + 2r$
Saddle $r \in (0, 1.81\dot{8}\dot{1})$
Unstable node $r > 1.81\dot{8}\dot{1}$

$(3,0)$: $\mu_1 = 1 - 6r$, $\mu_2 = 1 + .9r$
Saddle $r \in (0, \frac{1}{3})$
Unstable node $r > \frac{1}{3}$

$(2.1, 1.98)$: $\mu = 1 + r(-0.21 \pm i\sqrt{2.0349})$,
$|\mu|^2 = 1 - 0.42r + 2.079r^2$
Stable spiral $r \in (0, 0.20\dot{2}\dot{0})$,
Unstable spiral $r > 0.20\dot{2}\dot{0}$

As can be seen, not only is the stability of the fixed points dependent on the parameter r but also their type. As the fixed point $(0,0)$ becomes unstable at $r = \frac{2}{3}$ the eigenvalue μ_1 of the scheme is -1 and so we might expect a period doubling flip bifurcation to occur. This is bourne out by the bifurcation diagram of Figure 6 which depicts a slice through the three dimensional bifurcation diagram on the plane $v = 0$. The period 2 orbit lies in the $v = 0$ plane since the eigenvector corresponding to μ_1 (and λ_1) is $(1,0)^T$.

Figure 6 shows an interesting consequence of our technique for locating fixed points (see the Appendix for details), namely that since the stable eigendirection of the saddle at $(3,0)$ lies in the $v = 0$ plane it has been detected and represented on the bifurcation diagram. Notice that when this saddle becomes an unstable node at $r = \frac{1}{3}$ again $\mu_1 = -1$ and so period doubling is observed. Figures 7 – 9 illustrate orbits of the solution in the (u, v) plane for three different values of r. Notice that in these pictures the saddle does not appear whereas the fixed point (and its bifurcation) does.

When the spiral becomes unstable the eigenvalues are complex and so a Hopf bifurcation occurs giving rise to a limit cycle as depicted in Figures 10 and 8. Whereas bifurcation to a period two solution is readily detectable in numerical calculations, bifurcation to a limit cycle will not be so obvious, especially in the vicinity of the bifurcation (in the parameter r) and in higher dimensional problems. Indeed the phenomenon of an artificial time iteration to steady-state, of a large system formed by spatial discretisation, which gets near to convergence before the residuals "plateau out" could actually be the result of a limit cycle.

Finally note that although no spurious fixed points are generated by the uler scheme higher order period solutions, stable or unstable, are possible. Such spurious solutions can have a drastic effect on the basins of attraction of the true fixed points as is illustrated in Figure 11 where it can be seen that the basins for $(0,0)$ and $(2.1, 1.98)$ which extend to $\pm\infty$ for the OD s are severely truncated, as well as becoming segmented. One period 2 solution of the uler scheme applied to these equations is given by

$$\left(\tfrac{3}{2} \pm \tfrac{1}{2}\sqrt{9 + 4/r}, 0\right) \tag{30}$$

which for $r = 0.1$, the case for Figure 11, take the values $(-2,0)$ and $(5,0)$ which both lie on the boundaries of the truncated basins of attraction. This illustration should cause particular concern since it occurs at a value of r which is well below the linearised stability limit of both fixed points.

The linearised stability regions for the two stable fixed points are summarised for all of the Runge-Kutta methods we are considering in Table 5. We will only consider one other of them in detail here, namely the Modified

u’ = u*(-3 + 4u -v/2 -u**2), v’ = v*(-2.1 +u)

Euler

iterates 1001 to 11000, v = 0.0000

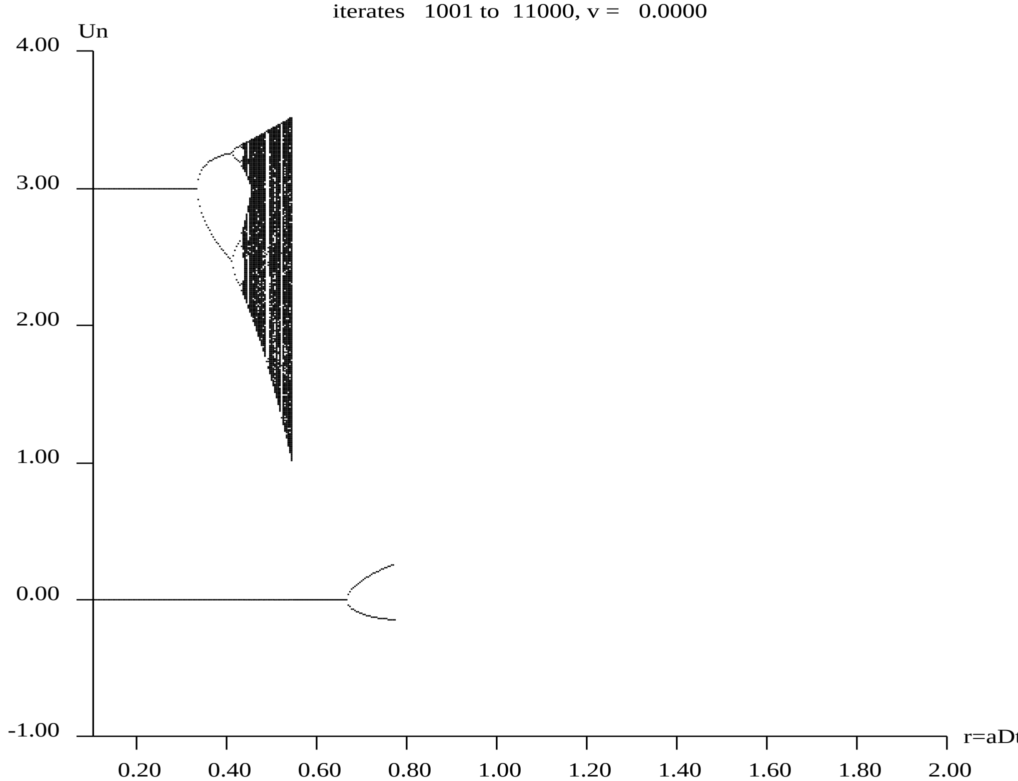

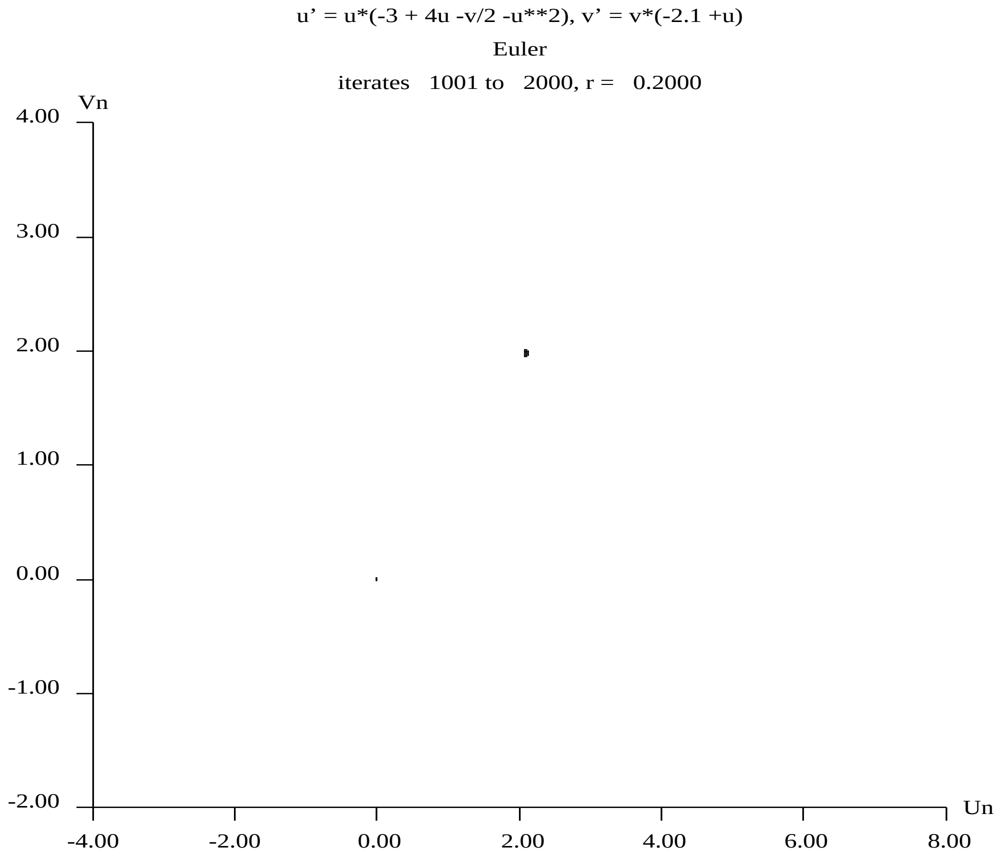

Figure 7: Phase orbits for the Predator Prey equations using the uler scheme.

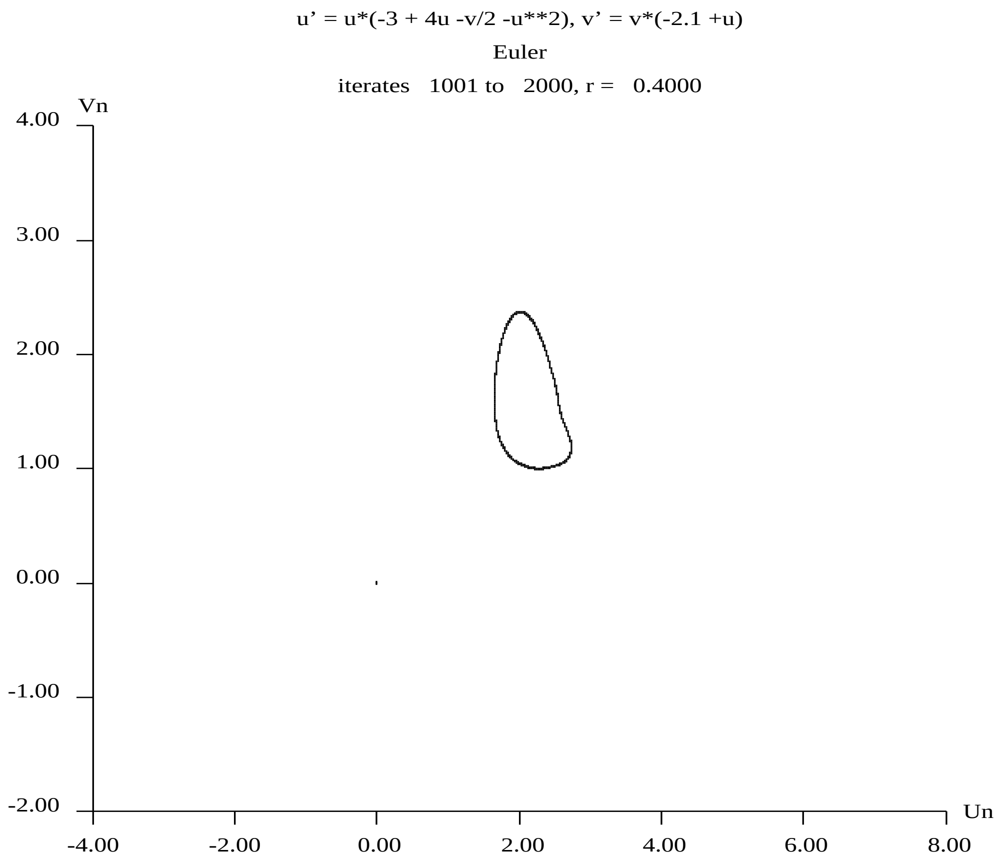

Figure 8: Phase orbits for the Predator Prey equations using the uler scheme $r = 0.4$.

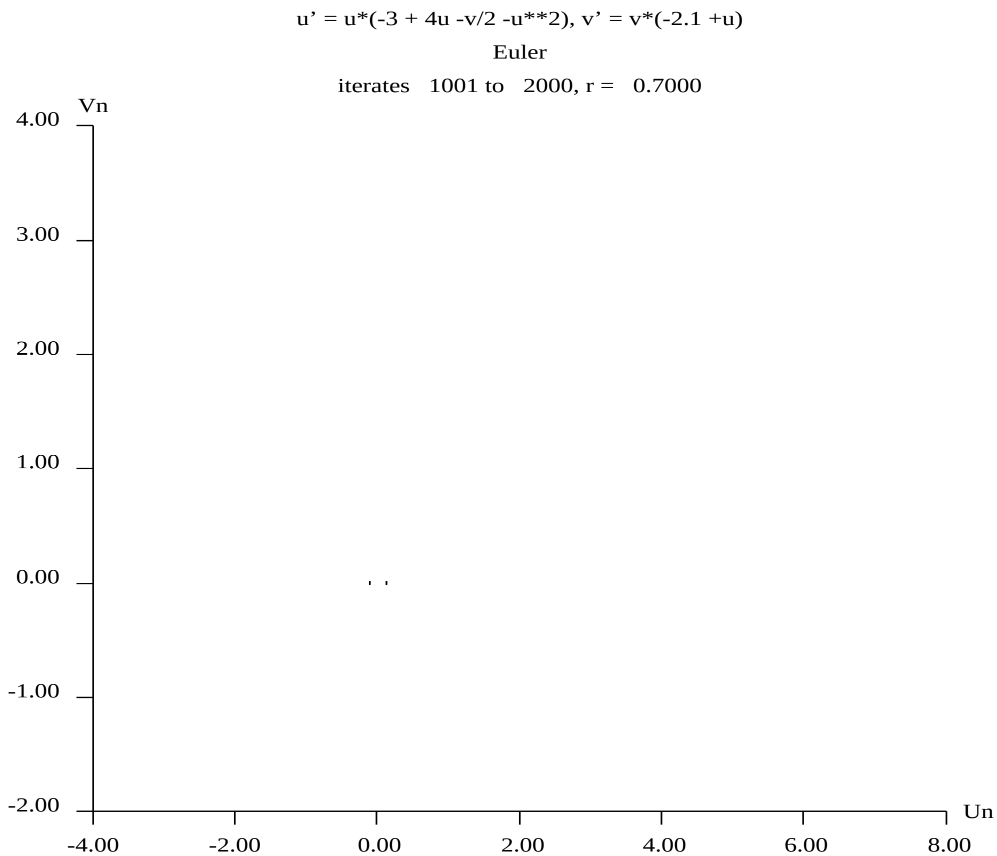

Figure 9: Phase orbits for the Predator Prey equations using the uler scheme $r = 0.7$.

u' = u*(-3 + 4u -v/2 -u**2), v' = v*(-2.1 +u)

Euler

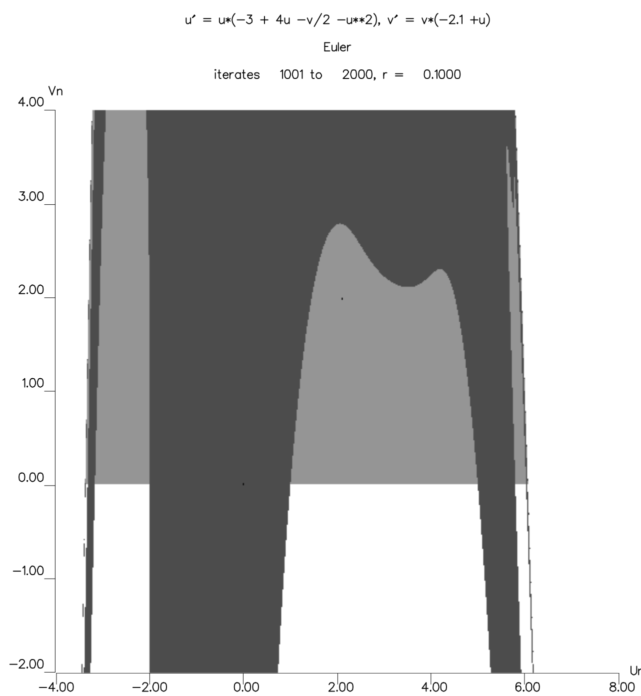

Figure 11: Basins of attraction for the Predator Prey equations using the uler scheme.

	$\frac{2}{3}$ $\frac{2}{3}$	

	S		[1]	E
	$\frac{3}{2}$ $\frac{1}{2}$ $\frac{3}{2}$ $\frac{1}{2}$ $\frac{1}{2}$ $\frac{1}{2}$ $\frac{1}{2}$ $\frac{1}{2}$		$\frac{2}{3}$	

E S

S $\frac{1}{2}$ S E

E

[1] E

$\frac{1}{2}$ [2] S E

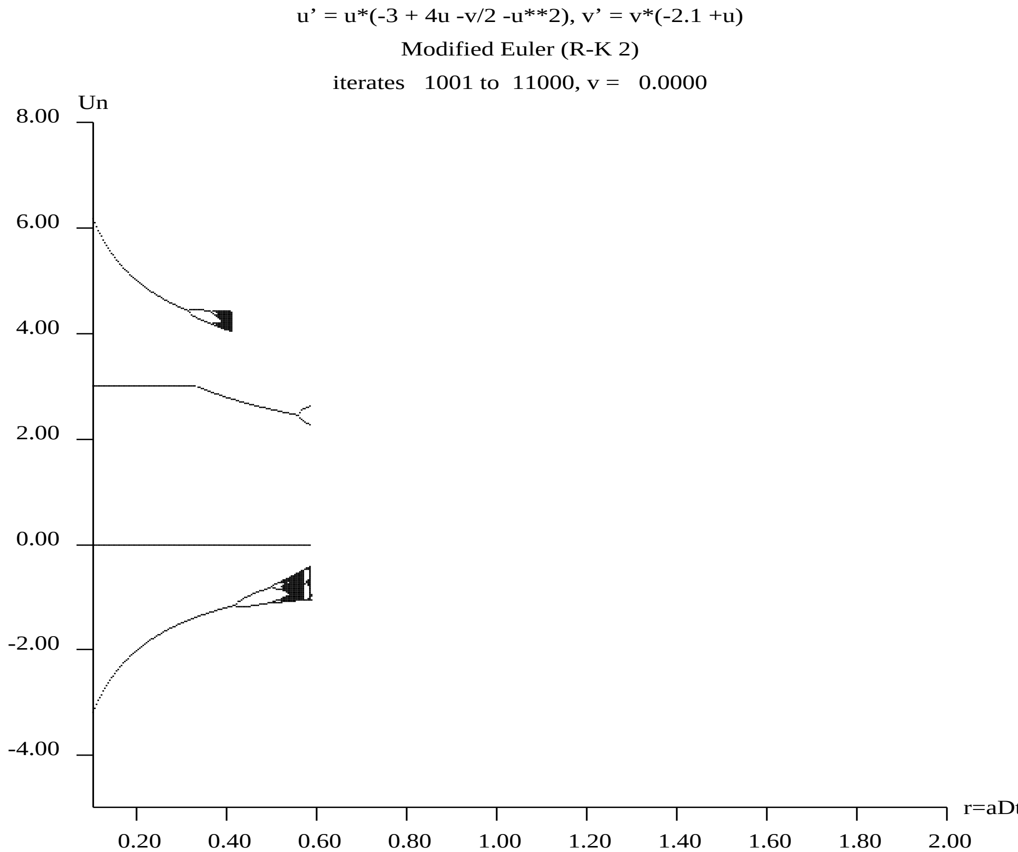
u' = u*(-3 + 4u -v/2 -u**2), v' = v*(-2.1 +u)
Modified Euler (R-K 2)
iterates 1001 to 11000, v = 0.0000
Un
8.00
6.00
4.00
2.00
0.00
-2.00
-4.00
0.20
0.40
0.60
0.80
1.00
1.20
1.40
1.60
1.80
2.00
r=aDt

u′ = u*(−3 + 4u −v/2 −u**2), v′ = v*(−2.1 +u)

Modified Euler (R–K 2)

iterates 100

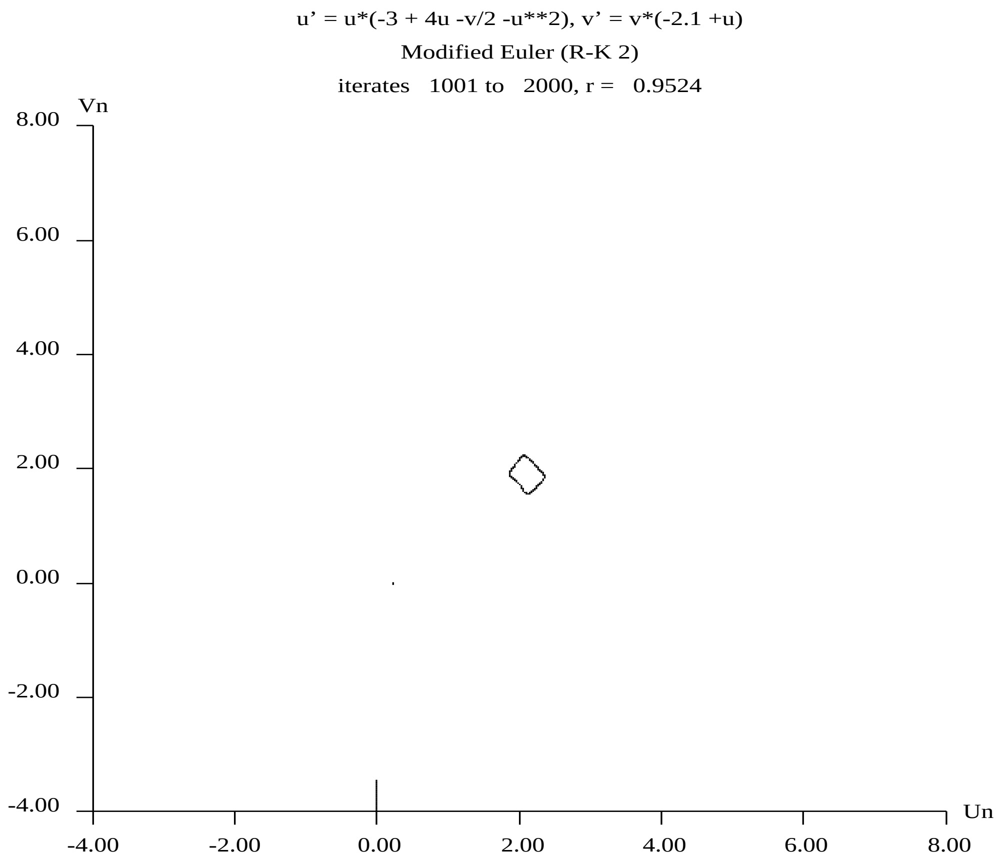

Figure 15: Spurious limit cycle for the Predator Prey equations using the Modified uler Scheme.

u’ = u*(-3 + 4u -v/2 -u**2), v’ = v*(-2.1 +u)

Improved Euler (R-K 2)

iterates   1001 to 11000, v =   0.0000

u’ = u*(-3 + 4u -v/2 -u**2), v’ = v*(-2.1 +u)

Heun (R-K 3)

iterates 1001 to 11000, v = 0.0000

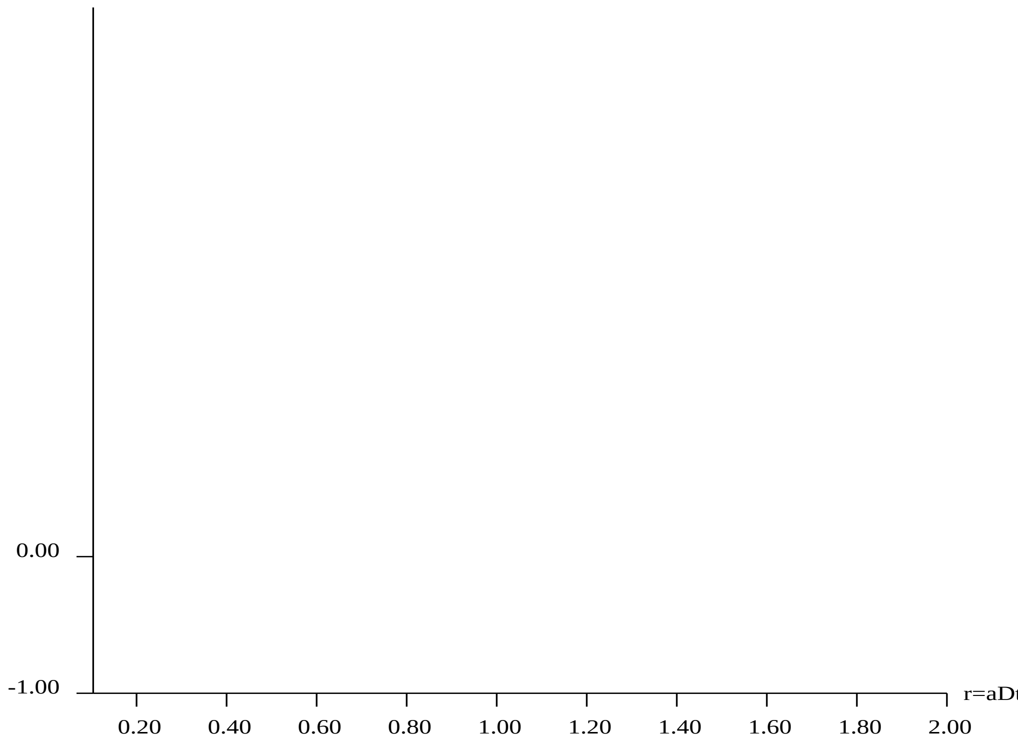

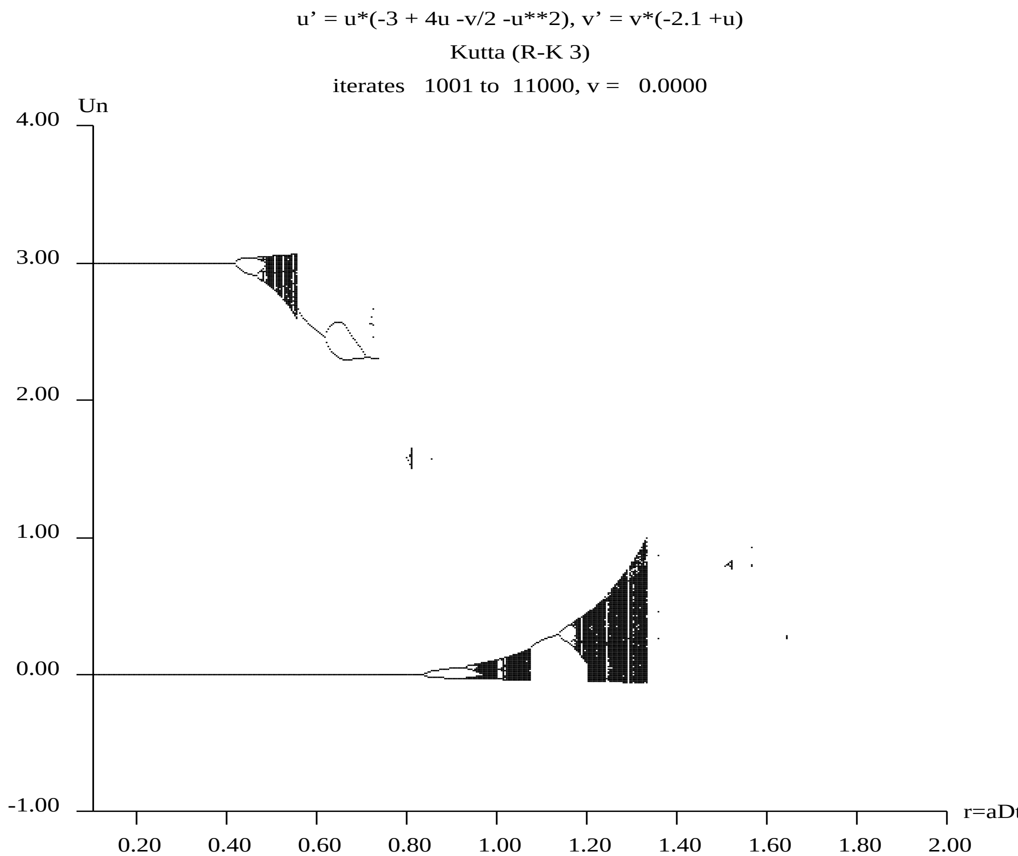

Figure 18: Bifurcation diagram for the Predator Prey equations using the Kutta scheme.

$u' = u*(-3 + 4u -v/2 -u**2), v' = v*(-2.1 +u)$

which is obviously the case here due to the appearance of the reciprocal of . For globally Lipschitz Humphries results states that spurious fixed points can not exist for arbitrarily small , again this is bourne out by our results for the Damped Pendulum equation.

If we apply the uler scheme (23) to the Damped Pendulum equation (11) we find, as expected, that the saddles at ((2 + 1) 0) remain saddles and that the type of the fixed points (when stable) at (0) are as for the OD , spirals for 2 and nodes for 2. Further more it is easy to obtain the linearised stability regions for these fixed points as being

$$(0 \quad) \qquad 2 \tag{32}$$

and

$$(0 \qquad \overline{\quad ^2 \quad 4)} \qquad 2 \tag{33}$$

We shall concentrate on the case 2 and look for period two solutions.

Period two solutions of the uler scheme must satisfy

$$(\ ) + \ (\ + \ (\ )) = 0 \qquad (\ ) = 0 \tag{34}$$

which for the Damped Pendulum equation becomes, after some manipulation,

$$\frac{\qquad ^2 \qquad}{\qquad}$$

$$\tfrac{1}{2} \ ^2 \qquad \tfrac{1}{2} \ ^2$$

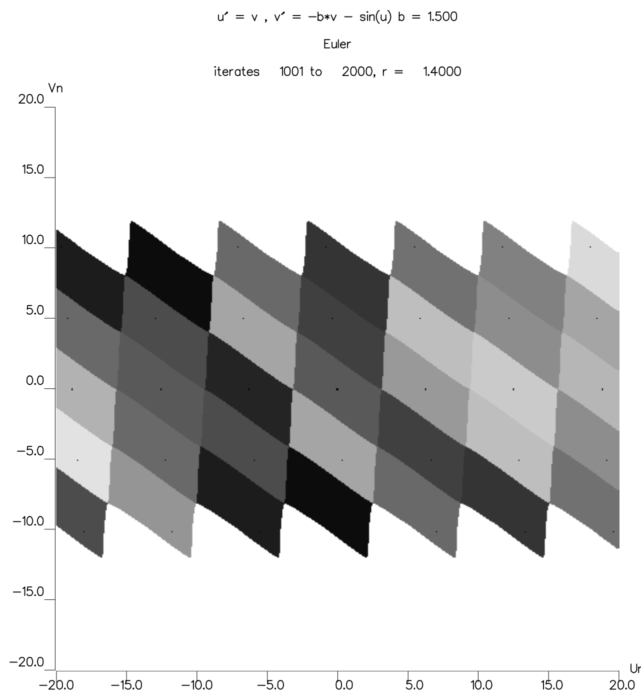

Figure 20: Subcritical period two solutions and their basins of attraction for the Damped Pendulum using the uler scheme.

u′ = v , v′ = −b*v − sin(u) b = 1.500

Euler

iterates 1001 to 2000, r = 1.6000

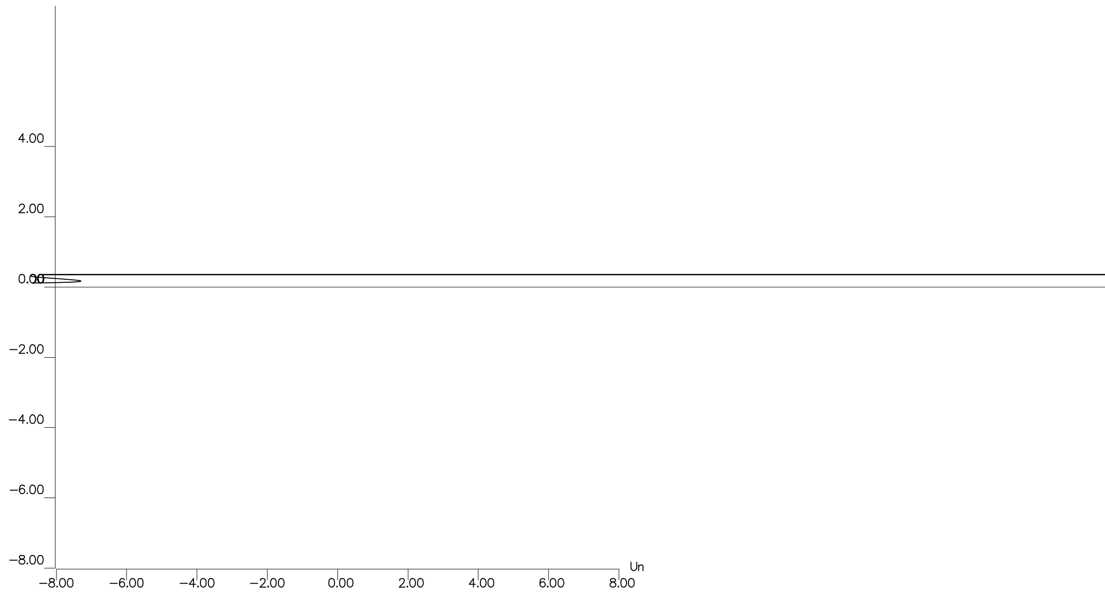

damped pendulum at (0,0)

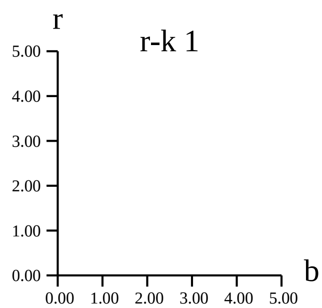

Figure 23: Spurious subcritical fixed points for the Damped Pendulum using the Modified uler scheme.

$$u' = v \; , \; v' = -b$$

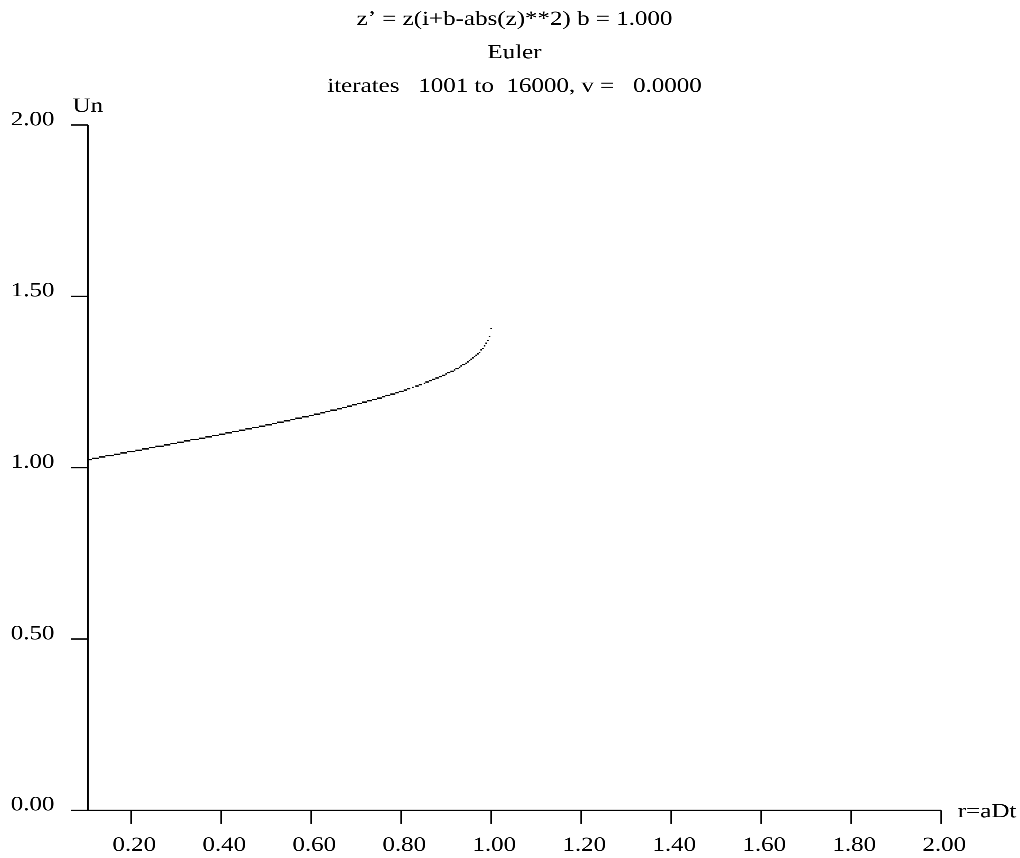

Figure 25: Bifurcation diagram of limit cycle for the Dissipative Complex equation produced by the uler scheme.

We consider only the case 0 where the OD has a limit cycle $=$ $-$.

k

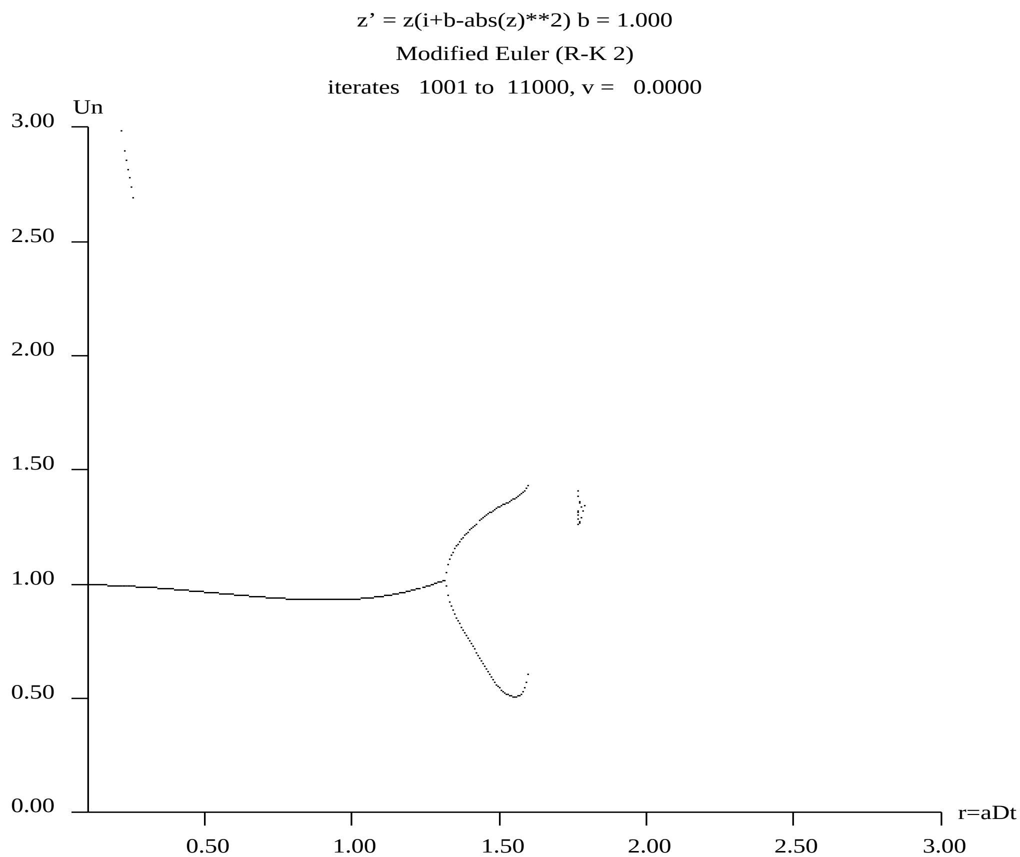

Figure 26: Bifurcation diagram of limit cycle for the Dissipative Complex equation produced by the Modified uler scheme.

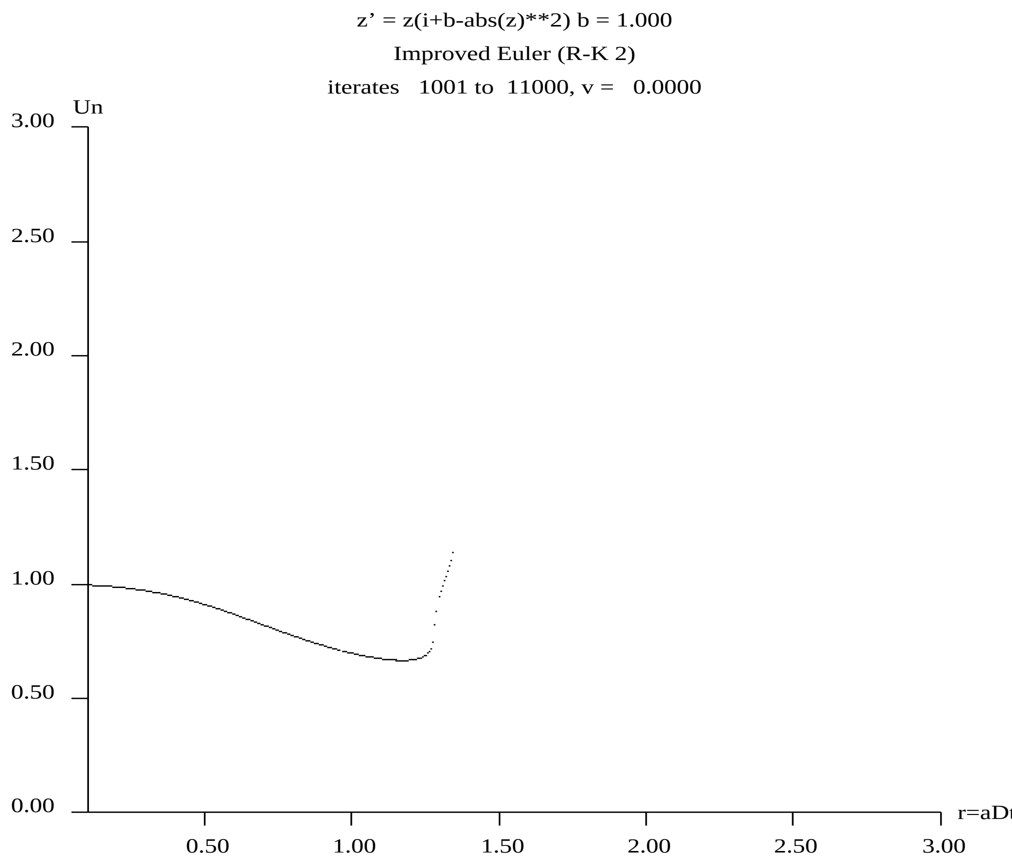

Figure 27: Bifurcation diagram of limit cycle for the Dissipative Complex equation produced by the Improved uler scheme.

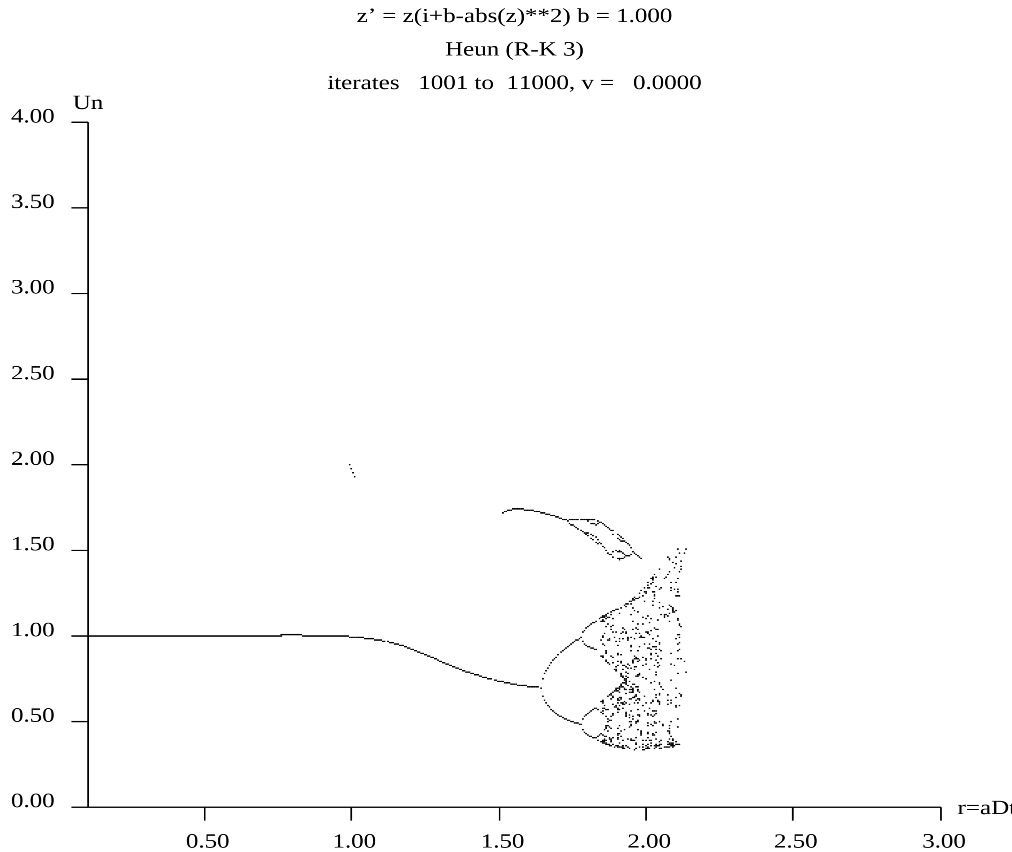

Figure 28: Bifurcation diagram of limit cycle for the Dissipative Complex equation produced by the Heun scheme.

z’ = z(i+b-abs(z)**2) b = 1.000

Runge-Kutta 4th order

iterates 1001 to 11000, v = 0.0000

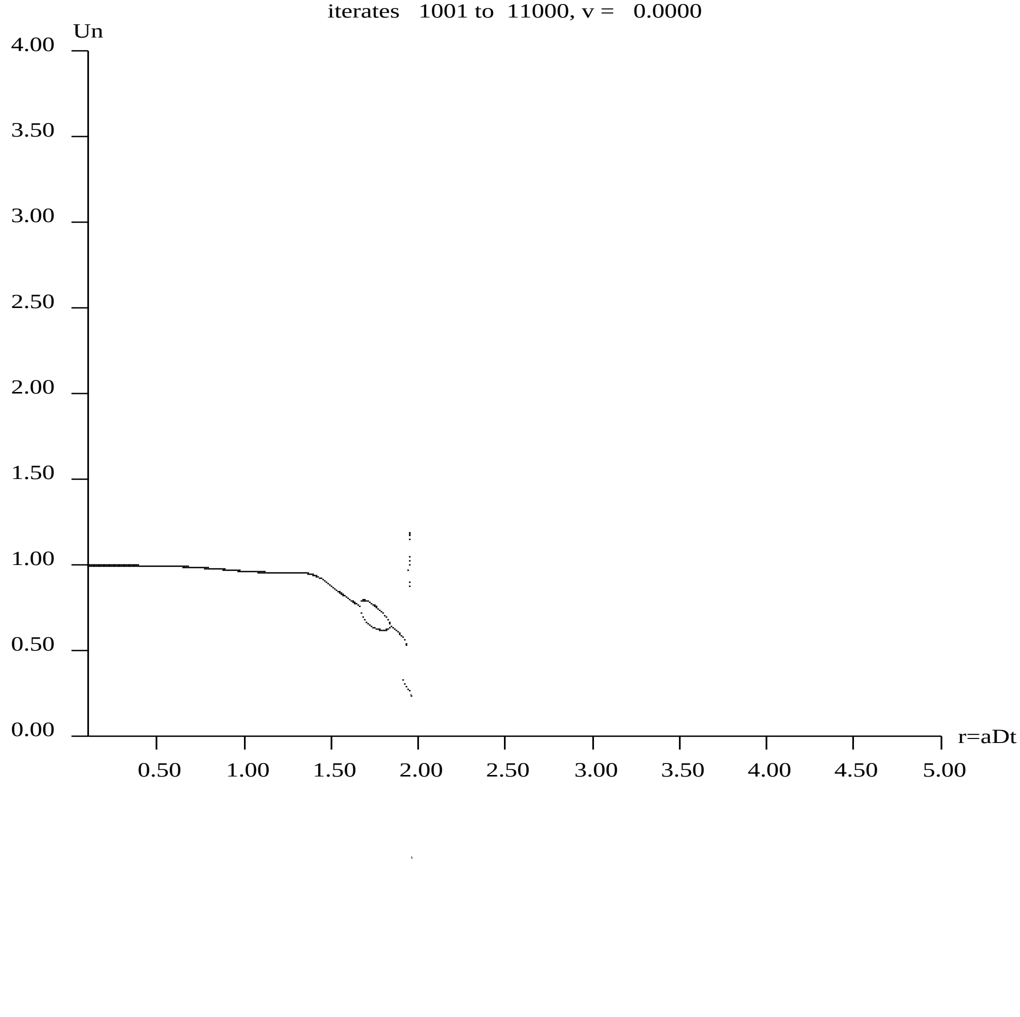

Perturbed Hamlitonian at (1/3,1/3)

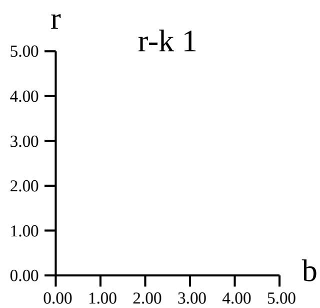

Figure 32: Section of bifurcation diagram for the Perturbed Hamiltonian using the Kutta scheme.

Figure 33: Spurious subcritical behaviour for the Perturbed Hamiltonian using the Kutta scheme.

- Spurious fixed points may be present both below and bifurcating from the linearised stablity limit of the essential fixed point of interest. In the former case the spuriousness of the limit point may not be recognised in complicated stituations and in the latter case the vicinity of the spurious limit point to the (now unstable) true limit point is likely to hide the misplacement in even simple cases.

- Stable and unstable spurious fixed points and higher order orbits drastically affect the basins of attraction of the essential fixed points of the OD s. As a consequence a lack of covergence or convergence to the wrong fixed point may occur. This is especially likely in the case of time-like iteration to steady-state where an arbitary initial condition is imposed.

- The bifurcation of spirals to limit cycles which might account, in part for the phenomenon of near (but lack of) convergence in large systems.

It should always be bourne in mind that although in our illustrations, due to their relatively simple nature and the manner of presentation of results (i.e. full representation of parameter space), the spurious dynamics has been readily detected; this will not always be the case in practical computations especially where higher order systems are involved.

6 Acknowledgements

We would like to thank David Griffiths (University of Dundee) and Andrew Stuart (University of Bath) for the many useful discussions during the course of this work and for suggesting the model equations (12) and (13).

Appendices

A omputations of orbits and bifuractions

The calculations carried out in this work were performed on a Connection Machine CM2 which is a parallel machine with 65,536 processors. The computational domain is considered as a 512×512 array of pixels, the value of the computational variables being taken at the center of each pixel.

The calculation of the bifurcation diagrams and the orbits is essentially the same, the only difference being the computational space $((r, u)$ or $(u, v))$ in which we are working. Initially the pixel variables are assigned values according to their position in computational space and constant v or r as appropriate. The numerical scheme is then applied to these values for an initial number of iterations (typically 1000) to allow the solution trajectories to reach their asymptotic states. At this stage the pixel variables will not have their initial (u, v) values, unless the pixel represents a fixed point or belongs to a periodic orbit. That is, if an initial value lies on a periodic orbit it will visit itself again at some later point in time. (A tolerance of half a pixel width is allowed, the initial number of iterations preventing mistaken identity of slowly varying trajectories.) Such points are marked on the raster display, and a further number of iterations taken, this time checking against initial conditions at each step, to identify all other such points. Due to the finite number of pixels and the form of the tolerance test high order periods will be detected, although they will appear as lower order periods due to the resolution.

The basins of attraction for both the bifurcation diagrams and the phase orbits are calculated in a similar manner by use of a reference point. For the bifurcation diagram case this point is $(r, u_{\min})$ where $u_{\min}$ is the minimum value of u on the orbit for which $v = 0$ and for the phase portraits the reference point is taken as $(u_{\min}, v(u_{\min}))$ where here $u_{\min}$ is the minimum value of u on the orbit. If the pixel values take the value of a reference point during the calculations then the pixel is coloured accordingly. (In practice the reference values are calculated at the same time being replaced whenever a point with smaller u value is found on the orbit.) Note that the reference values must belong to the orbits and so are found using the same techniques as above.

References

[1] Abraham, R.H. Shaw, C.D. *Dynamics The eometry of Behaviour (3 vols)*Aerial Press, Snata Cruz, CA 1982,3,5

[2] Andronov, A.A., Leontovich, .A., Gordon, I.I. and Maier A.G. *Theory of Bifurcations of Dynamic Systems on a Plan,* Israel Program for Scientific Translations Ltd., 1971, U.S. Department of Commerce, National Information Service, Springfield, Va. 22151.

[3] Andronov, A.A., Leontovich, .A., Gordon, I.I. and Maier A.G. *Qualitative Theory of Second-Order Dynamic Systems,*A. Halsted press book, John Wiley Sons, New York, 1973.

[4] Chow, S.N. Hale, J.K. *Methods of Bifurcation Theory,* Springer–Verlag 1982

[5] D RIV Computer algebraic manipulation package.

[6] Griffiths, D.F., Stuart, A.M. Yee, H.C.
University of Bath
Report, March 1991

[7] Griffith, D.F., Sweby, P.K. Yee, H.C.
to appear IMA J. Numer.
Anal.

[8] Guckenheimer, J. Holmes, P.
Springer–Verlag 1983

[9] Hairer, ., Iserles, A. Sanz-Serna, J.M.
1989, to appear NUmer. Math.

[10] Humphries, A.R.
Submitted IMA J. Num. Anal. 1991

[11] Iserles, A.
IMA J. Numer. Anal., 1990

[12] Lafon, A. Yee, H.C.
NASA TM 103877, July 1991

[13] Lafon, A. Yee, H.C.
NASA TM
in preparation 1991

[19] Yee, H.C., Sweby, P.K. Griffiths, D.F. *Dynamical Approach Study of Spurious Steady-State Numerical solutions for Nonlinear Differential Equations, Part I, The Dynamics of Time Discretizations and its Implications for Algorithm Development in Computational Fluid Dynamics,* NASA TM 102820, April 1990, to appear J. Comput. Phys., 1991